Condensed Matter Physics 2007, Vol. 10, No 1(49), pp. 85–89

Pyroelectric response of inhomogeneous ferroelectric-semiconductor films

A.N.Morozovska*

V.Lashkaryov Institute of Semiconductor Physics of the National Academy of Sciences of Ukraine, Ave. Nauki 41, 03028 Kiev, Ukraine

Received September 4, 2006, in final form November 17, 2006

We have modified Landau-Khalatnikov approach and shown that the pyroelectric response of inhomogeneous ferroelectric-semiconductor films can be described by using six coupled equations for the average displacement, its mean-square fluctuation and correlation with charge defects density fluctuations, average pyroelectric coefficient, its fluctuation and correlation with density fluctuations of charged defects.

Coupled equations demonstrate the inhomogeneous reversal of pyroelectric response in contrast to the equations of Landau-Khalatnikov type, which describe the homogeneous reversal with sharp pyroelectric coefficient peaks near the thermodynamic coercive field values. Our approach explains pyroelectric loops observed in $Pb(Zr,Ti)O_3$ film.

Key words: *ferroelectric-semiconductor film, pyroelectric response, charged defects*

PACS: *77.80.-e, 77.84.Dy, 68.03.Cd, 68.35.Gy*

1. Introduction

The main peculiarity of ferroelectric materials is hysteresis dependence of their dielectric permittivity ε, spontaneous displacement D and pyroelectric coefficient γ on electric field E_0 applied to the sample [1]. The pyroelectric hysteresis loops of inhomogeneous ferroelectric-semiconductor films have several characteristic features depicted in figure 1a.

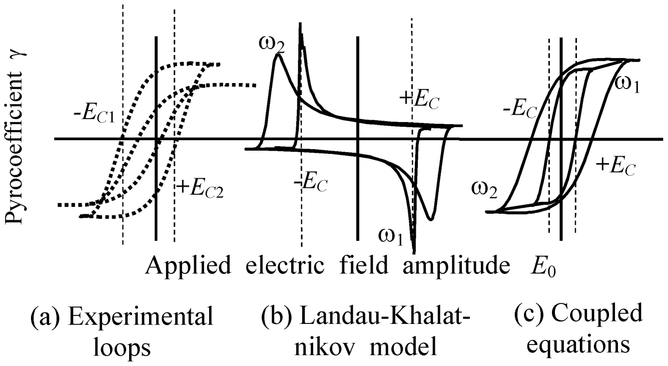

Figure 1. Pyroelectric $\gamma\,(E_0)$ hysteresis loops. Different plots correspond to the data obtained for a semiconductor-ferroelectric film (a), Landau-Khalatnikov model (b) and our coupled equations (c) for a bulk sample ($\omega_1 \ll \omega_2$ are two frequencies of the applied electric field).

Such typical ferroelectric-semiconductors as slightly doped $Pb(Zr,Ti)O_3$ solid solutions, their films, multilayers and heterostructures are widely used in actuators, electro-optic, piezoelectric, pyroelectric sensors and memory elements [2–4]. However, the task of creating the ferroelectric

*E-mail: morozo@i.com.ua

material with pre-determined dielectric and/or pyroelectric properties is solved mainly empirically. The correct theoretical consideration could answer fundamental questions as well as help to tailor new ferroelectric-semiconductor materials, save time and expenses.

Conventional phenomenological approaches with material parameters obtained from first-principle calculations give significantly incomplete picture of the pyroelectric hysteresis in the doped or inhomogeneous ferroelectrics-semiconductors (compare figure 1b with figure 1a). In particular, Landau-Khalatnikov approach, evolved for the single domain perfect ferroelectrics-dielectrics, describes homogeneous polarization reversal but does not describe the domain nucleation and movement [5,6]. Therefore, its modification for inhomogeneous ferroelectrics-semiconductors seems necessary [7,8].

In our recent papers [9–12] we have considered the displacement fluctuations caused by charged defects and modified the Landau-Khalatnikov approach for the inhomogeneous ferroelectrics-semiconductors. In this paper we develop the proposed model for pyroelectric response (see figure 1c).

2. Coupled equations

Let us consider n-type ferroelectric-semiconductor with sluggish randomly distributed defects. The charge density of defects $\rho_s(\mathbf{r})$ is characterized by the positive average value $\bar{\rho}_{\mathrm{S}}$ and random spatial fluctuations $\delta\rho_{\mathrm{S}}(\mathbf{r})$, i.e. $\rho_{\mathrm{S}}(\mathbf{r}) = \bar{\rho}_{\mathrm{S}} + \delta\rho_{\mathrm{S}}(\mathbf{r})$ (the dash designates average values). The average distance between quasi-homogeneously distributed defects is d. Screening clouds $\delta n(\mathbf{r},t)$ with Debye screening radius R_{D} surround each charged center, so the free carriers charge density is $n(\mathbf{r},t) = \bar{n} + \delta n(\mathbf{r},t)$. Screening clouds are deformed in the external field E_0, and the system "defect center $\delta\rho_{\mathrm{S}}$ + screening cloud δn" causes displacement fluctuations $\delta D(\mathbf{r},t)$ in accordance with Maxwell's equations $\operatorname{div}\mathbf{D} = 4\pi\,(n+\rho_{\mathrm{S}})$, $\operatorname{div}(\partial\mathbf{D}/\partial t + 4\pi\,\mathbf{j}_{\mathrm{c}}) = 0$ (see figure 2).

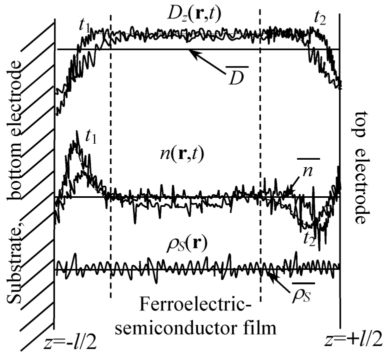

Figure 2. Spatial distribution of displacement $D(\mathbf{r},t_{1,2})$, free carriers charge density $n(\mathbf{r},t_{1,2})$ and sluggish defects density ρ_S in an inhomogeneous ferroelectric-semiconductor film.

In this way we obtained six coupled equations for the average displacement $\overline{D}$, its mean-square fluctuation $\overline{\delta D^2}$ and correlation $\overline{\delta D\,\delta\rho_{\mathrm{S}}}$, pyroelectric coefficient $\bar{\gamma} = \partial\bar{D}/\partial T$, its deviation $\overline{\delta\gamma} = \partial\,\overline{\delta D^2}\Big/\partial T$ and correlation with charge defects density fluctuations $\overline{\delta\gamma\,\delta\rho_{\mathrm{S}}} = \partial\,\overline{\delta D\,\delta\rho_{\mathrm{S}}}/\partial T$ (see [13]):

$$\Gamma\frac{\partial\bar{D}}{\partial t} + \left(\alpha + 3\,\beta\,\overline{\delta D^2}\right)\,\bar{D} + \beta\bar{D}^3 = E_0(t) + E_i(l,t), \tag{1}$$

$$\frac{\Gamma_{\mathrm{R}}}{2}\frac{\partial\,\overline{\delta D^2}}{\partial t} + \left(\alpha_{\mathrm{R}} + 3\beta\bar{D}^2\right)\,\overline{\delta D^2} + \beta\left(\overline{\delta D^2}\right)^2 = \left(E_0(t)\left(\frac{\overline{\delta D\,\delta\rho_{\mathrm{S}}}}{\bar{n}} - \delta E_i\right) + \frac{4\pi k_{\mathrm{B}}T}{\bar{n}e}\overline{\delta\rho_{\mathrm{S}}\,(\delta\rho_{\mathrm{S}}+\delta n)}\right), \tag{2}$$

$$\Gamma_{\mathrm{R}}\frac{\partial\,\overline{\delta D\,\delta\rho_{\mathrm{S}}}}{\partial t} + \left(\alpha_{\mathrm{R}} + 3\,\beta\bar{D}^2 + \beta\,\overline{\delta D^2}\right)\;\overline{\delta D\,\delta\rho_{\mathrm{S}}} = -E_0(t)\frac{\overline{\delta\rho_{\mathrm{S}}\delta n}}{\bar{n}}. \tag{3}$$

$$\Gamma\frac{\partial\,\bar{\gamma}}{\partial t} + \left(\alpha + 3\,\beta\,\overline{\delta D^2} + 3\beta\bar{D}^2\right)\,\bar{\gamma} = -\left(\alpha_{\mathrm{T}} + 3\,\beta\;\overline{\delta\gamma^2}\right)\,\bar{D}, \tag{4}$$

$$\begin{aligned}\Gamma_{\mathrm{R}}\frac{\partial\overline{\delta\gamma\,\delta D}}{\partial t} + 2\left(\alpha_{\mathrm{R}} + 2\,\beta\,\overline{\delta D^2} + 3\,\beta\,\bar{D}^2\right)\,\overline{\delta\gamma\,\delta D} = \Bigg(&E_0(t)\frac{\overline{\delta\gamma\,\delta\rho_{\mathrm{S}}}}{\bar{n}} - \left(\alpha_{\mathrm{RT}} + 6\,\beta\,\bar{D}\,\bar{\gamma}\right)\;\overline{\delta D^2}\\ &+ \frac{4\pi k_{\mathrm{B}}}{\bar{n}e}\overline{\delta\rho_{\mathrm{S}}\,(\delta\rho_{\mathrm{S}}+\delta n)}\Bigg),\end{aligned} \tag{5}$$

$$\Gamma_{\mathrm{R}}\frac{\partial\,\overline{\delta\gamma\,\delta\rho_{\mathrm{S}}}}{\partial t} + \left(\alpha_{\mathrm{R}} + \beta\,\overline{\delta D^2} + 3\,\beta\,\bar{D}^2\right)\;\overline{\delta\gamma\,\delta\rho_{\mathrm{S}}} = -\left(\alpha_{\mathrm{RT}} + 2\beta\,\overline{\delta\gamma\,\delta D} + 6\,\beta\,\bar{D}\,\bar{\gamma}\right)\;\overline{\delta D\,\delta\rho_{\mathrm{S}}}\quad. \tag{6}$$

The built-in electric field

$$E_i\left(l,t\right)=\frac{4\pi\gamma}{l}\,\overline{\left(\delta n\left(t\right)+\delta\rho_{\mathrm{S}}\right)_{x,y}}\Big|_{-l/2}^{+l/2}$$

in (1) and its deviation

$$\delta E_i=\frac{2\pi}{l\,\bar{n}}\,\overline{\left(\int\limits_{z_0}^{z}\mathrm{d}z\left(\delta n+\delta\rho_{\mathrm{S}}\right)\right)^2_{x,y}}\Bigg|_{-l/2}^{+l/2}$$

in (2) are inversely proportional to the film thickness l, thus it vanishes in the bulk material. For a finite film it is induced by the space charge layers accommodated near the non-equivalent boundaries $z=\pm l/2$ of the examined heterostructure/multilayer (e.g. near the substrate with bottom electrode and free surface with top electrode depicted in figure 2). Such layers are created by the screening carriers [5–7]. In general case the field $E_i\left(l,\,t\right)$ can be time-dependent, its amplitude is proportional to the space charge fluctuations $|\delta n+\delta\rho_{\mathrm{S}}|$. Also E_i diffuses paraelectric-ferroelectric phase transition. In particular, it shifts and smears dielectric permittivity temperature maximum.

Bratkovsky and Levanyuk [8] predicted the existence of built-in field in a finite ferroelectric film within the framework of phenomenological consideration. Our approach confirms their assumption and gives the expression of the field existing in the inhomogeneous ferroelectric-semiconductor film.

Renormalization $\Gamma_{\mathrm{R}}\equiv\Gamma+\tau_m$ of Khalatnikov kinetic coefficient is connected with the contribution of free carrier Maxwellian relaxation. The renormalization of coefficients $\alpha_{\mathrm{R}}\equiv\alpha+\left(\gamma+k_{\mathrm{B}}T/4\pi\,\bar{n}e\right)\big/d^2$ and $\alpha_{\mathrm{RT}}\equiv\alpha_{\mathrm{T}}+k_{\mathrm{B}}\big/4\pi\,\bar{n}ed^2$ is connected with the contribution of correlation and screening effects [9,13]. Coefficient $\alpha=-\alpha_{\mathrm{T}}(T_{\mathrm{C}}-T)$ is negative in the perfect ferroelectric phase without random defects ($\overline{\delta\rho^2_{\mathrm{S}}}=0$). For the partially disordered ferroelectric with charged defects ($\overline{\delta\rho^2_{\mathrm{S}}}>0$) coefficient α_{R} is positive and $\alpha_{\mathrm{R}}\gg|\alpha|$, $\alpha_{\mathrm{RT}}\gg\alpha_{\mathrm{T}}$. For example, for Pb(Zr,Ti)O_3 solid solution $\alpha\sim-\left(0.4\div2\right)\cdot10^{-2}$ [3], gradient term $\lambda\approx5\cdot10^{-16}$ cm^2, screening radius $R_{\mathrm{D}}\sim\left(10^{-6}\div10^{-4}\right)$ cm [5], average distance between defects $d\sim\left(10^{-6}\div10^{-4}\right)$ cm and thus $\alpha_{\mathrm{R}}\sim1\div10^2$. So the ratio $\xi=-\alpha_{\mathrm{R}}/\alpha\approx\alpha_{\mathrm{RT}}T/\alpha_{\mathrm{T}}(T_{\mathrm{C}}-T)$ is greater than 100.

The dimensionless amplitude $g=4\pi k_{\mathrm{B}}T\cdot\bar{n}\big/\left(-\alpha D^2_{\mathrm{S}}e\right)$ of displacement fluctuations $\overline{\delta\rho_{\mathrm{S}}\left(\delta\rho_{\mathrm{S}}+\delta n\right)}$ varies in the range from 10^2 to10^4 for Pb(Zr,Ti)O_3 ($D_{\mathrm{S}}=\sqrt{-\alpha/\beta}$). The positive correlator $R^2\left(t\right)=-\,\overline{\delta\rho_{\mathrm{S}}\delta n\left(t\right)}\big/\bar{n}^2$ was calculated in [9] at small external field amplitude and low frequency. Under the condition of prevailing extrinsic conductivity $\bar{n}\approx-\bar{\rho}_{\mathrm{S}}$ the correlator $R^2\left(\,t\right)$ varies in the range (0; 1) because its amplitude is proportional to the charged defects disordering $\overline{\delta\rho^2_{\mathrm{S}}}\big/\bar{\rho}^2_{\mathrm{S}}$.

Hereinafter we discuss only the pyroelectric response near the equilibrium states. The system (1)–(6) quasi-equilibrium behavior is described by the dimensionless built-in field amplitude$E_m=E_i/E_{\mathrm{C}}\sim\left(\delta n+\delta\rho_{\mathrm{S}}\right)$ and frequency $w=-\Gamma\omega/\alpha$ as well as by the aforementioned parameters ξ, $R^2\left(w\right)$,g and temperature T/T_{C} ($E_{\mathrm{C}}=-\alpha\sqrt{-\alpha/\beta}$). Under the conditions $w<1$, $g\gg1$ and $\xi\gg1$ the scaling parameter $gR^2\big/\xi$ determines the system behavior [9].

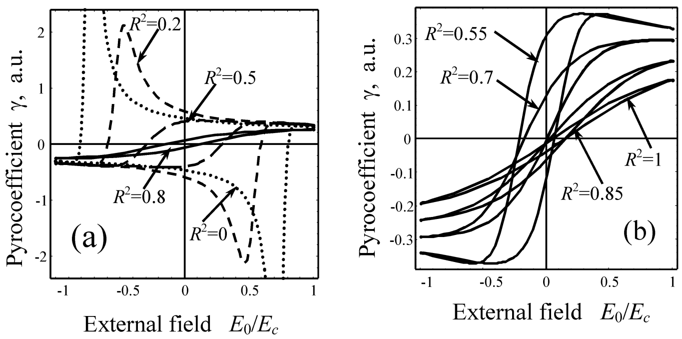

Figure 3. Hysteresis loops of pyroelectric coefficient $\overline{\gamma\left(E\right)}$ for different R^2 values. Other parameters: $g=100$, $\xi=100$, $T/T_C=0.45$, $w=0.05$ and $E_i=0$ (plot (a) for the bulk sample) and $E_i=\pm0.1\cdot R$, (plot (b) for the film).

Figure 3 demonstrates the typical changes of pyroelectric hysteresis loop caused by the increase of charged defects disordering (note, that $gR^2/\xi \sim \overline{\delta\rho_S^2}\big/\bar{\rho}_S^2$). It is clear that the increase of gR^2/ξ value leads to the essential decrease and smearing of pyroelectric coefficient peaks near the coercive field as well as to the decrease of the coercive field value (compare Landau-Khalatnikov loops ($R^2 = 0$) with dashed curves ($R^2 \geqslant 0.2$)).

Let us underline that we do not know any experiment, in which pyroelectric coefficient peaks near the coercive field have been observed. Moreover, usually pyroelectric hysteresis loops in doped ferroelectrics have a typical “slim” shape with coercive field values much lower than the thermodynamic one [14,15]. The quantitative comparison of our results with typical PZT-pyroelectric loops is presented in the next section.

2.1. Discussion

Dopants, as well as numerous unavoidable oxygen O^{-2} vacancies, can play a role of randomly distributed charged defects in “soft” PZT. In this case ferroelectric and pyroelectric hysteresis loops have got relatively high γ and D remnant values, but reveal low coercive fields [3]. Usually pyroelectric hysteresis loops of PZT are rather slim and sloped even at low frequencies $\omega \sim (0.1 \div 10)Hz$ [3], no pyroelectric coefficient maximum near the coercive field is observed [14–16].

The pyroelectric response of the PZT films was registered by means of dynamic pyroelectric measurements (see [14,16] for details). During the measurements, the quasi-static voltage Uvaried in the range (–11V, +11V) at the low-frequency $\omega \sim 0.01\ Hz$, the temperature T changes near the room temperature with the frequency about 20 Hz. Pyroelectric hysteresis loops for $U_{\pi\,1} \sim \bar{\gamma}$ and $U_{\pi\,2} \sim \bar{\gamma}/\bar{\varepsilon}$ are presented in figures 4.

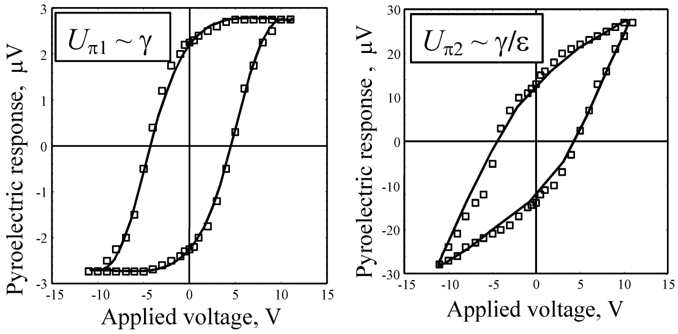

Figure 4. Pyroelectric hysteresis loops ($U_{\pi 1} \sim \bar{\gamma}$ and $U_{\pi 2} \sim \bar{\gamma}/\bar{\varepsilon}$) of 1.9 μm-thick PZT(46/54): Nb film. Squares are experimental data measured by Bravina *et al.* [14], solid curves are our calculation with the fitting parameters $w = 0.1$, $R^2 = 0.5$, $g = 100$, $\xi = 100$, $E_m = -0.03$.

It is clear from the figures that our model both qualitatively and quantitatively describes pyroelectric hysteresis loops in thick “soft” PZT films. The modelling of ferroelectric and dielectric hysteresis loops was performed earlier (see e.g. [9]).

Earlier we proved [9–13] that the effect of random defect leads to the non-zero average values of $\overline{\delta D^2}$ even at $\bar{D} = 0$. This means that the sample is divided into polar regions with opposite polarization, i.e. the domain structure originates from charged defects. In our model we neither consider the spatial distribution of the emerged domain structure nor incorporate its initial distribution. We calculate the average values only. The initial distribution of polar regions determines the initial conditions of the system (1)–(6), which do not affect the equilibrium hysteresis loop shape [9].

Surely, the domain formation can be caused by many other factors besides the considered charged defects, e.g. by local inhomogeneous stresses and elastic defects. In particular, the presence of elastic defects or other pinning centers undoubtedly causes additional domain splitting, domain walls movement and pinning. Allowing for piezoelectric effect, the displacement fluctuations caused by random elastic defects could be included in the system of coupled equations. Thus, one could assume that their contribution leads to additional smearing of hysteresis loop, changes the coercive field and saturation law at high external fields [1].

Thus, the modelling based on the coupled equations (1)–(6) gives realistic coercive field values and a typical pyroelectric hysteresis loop shape. Taking into account that the inhomogeneous reversal of spontaneous polarization and pyroelectric response occurs in the doped or inhomogeneous ferroelectrics-semiconductors, the proposed coupled equations could be more relevant in the phenomenological description of their pyroelectric properties than the models based on Landau-Khalatnikov phenomenology.

References

1. Lines M.E., Glass A.M. Principles and Applications of Ferroelectrics and Related Phenomena. University Press, Oxford, 1978.
2. Lang S.B. Physics Today, 2005, **58**(8), 31–36.
3. Cross L.E. Ferroelectric Ceramics: Tailoring Properties for Specific Application. Birkhauser Verlag, Basel, 1993.
4. Scott J.F. Ferroelectric Memories. Springer, Berlin and Heidelberg, 2000.
5. Fridkin V.M. Ferroelectrics Semiconductors. Consultant Bureau, New-York and London, 1980.
6. Sandomirskii V.B., Khalilov Sh.S., Chenskii E.V. Physics and technics of semiconductors, 1982, **16**, 440.
7. Baudry L., Tournier J. J. Appl. Phys., 2005, **97**, 024104–11.
8. Bratkovsky A.M., Levanyuk A.P. Phys. Rev. Lett., 2005, **94**, 107601–4.
9. Morozovska A.N., Eliseev E.A. J. Phys.: Condens. Matter., 2004, **16**, 8937–8956; Preprint cond–mat/0408647.
10. Morozovska A.N., Eliseev E.A. Physica B, 2005, **355**, 236–243.
11. Morozovska A.N., Eliseev E.A. Phys. Stat. Sol. (b), 2005, **242**, 947–961.
12. Morozovska A.N. Ferroelectrics, 2005, **317**, 37–42.
13. Morozovska A.N., Eliseev E.A., Remiens D., Soyer C. J. Appl. Phys., 2006, **100**, 014109–1–12.
14. Bravina S.L., Cattan E., Morozovsky N.V., Remiens D. Semiconductor Physics, Quantum Electronics & Optoelectronics, 2004, **7**, 263–271.
15. Kostsov E.G. Ferroelectrics, 2005, **314**, 169–187.
16. Haccart T., Cattan E., Remiens D. Semiconductor Physics, Quantum Electronics & Optoelectronics, 2002, **5** (1), 78–88.

Піроелектричний відгук неоднорідних сегнетоелектрично-напівпровідникових плівок

Г.М.Морозовська

Інститут фізики напівпровідників ім. В. Лашкарьова, НАН України, пр. Науки 41, 03028 Київ, Україна

Отримано 4 вересня 2006 р., а остаточному вигляді – 17 листопада 2006 р.

Модифіковано підхід Ландау-Халатнікова та показано, що піроелектричний відгук неоднорідної сегнетоелектрично-напівпровідникової плівки з зарядженими дефектами може бути описаний за допомогою шести зв'язаних рівнянь для шести параметрів порядку: середня електрична індукція, її середньоквадратичне відхилення, корелятор флуктуацій індукції та густини заряду дефектів, піроелектричний коефіцієнт, його середньоквадратичне відхилення та корелятор з густиною заряду дефектів.

Зв'язані рівняння описують неоднорідне переключення піроелектричного відгуку на відміну від рівнянь типу Ландау-Халатнікова, які відповідають випадку однорідного переключення з різким максимумом піроелектричного відгуку поблизу коерцитивного поля. Запропонована модель пояснює типові петлі піроелектричного гістерезису у $Pb(Zr,Ti)O_3$ плівках.

Ключові слова: *плівка сегнетоелектрика-напівпровідника, піроелектричний відгук, заряджені дефекти*

PACS: *77.80.-e, 77.84.Dy, 68.03.Cd, 68.35.Gy*